High resolution photodetachment spectroscopy of negative ions via slow photoelectron imaging

Andreas Osterwalder, Matthew J. Nee, Jia Zhou, and Daniel M. Neumark[a)]
Department of Chemistry, University of California, Berkeley, California 94720 and Chemical Sciences Division, Lawrence Berkeley National Laboratory, Berkeley, California 94720

(Received 15 June 2004; accepted 8 July 2004)

A technique for high resolution anion photodetachment spectroscopy is presented that combines velocity map imaging and anion threshold photodetachment. This method, slow electron velocity-map imaging, provides spectral line widths of better than 1 meV. Spectra over a substantial range of electron kinetic energies are recorded in a single image, providing a dramatic reduction of data acquisition time compared to other techniques with comparable resolution. We apply this technique to atomic iodine and the van der Waals cluster $I \cdot CO_2$ as test systems, and then to the prereactive $Cl \cdot D_2$ complex where partially resolved structure assigned to hindered rotor motion is observed. © *2004 American Institute of Physics.* [DOI: 10.1063/1.1787491]

I. INTRODUCTION

Photoelectron spectroscopy (PES) of anions is a very powerful method for the determination of electron affinities and the study of exotic species such as reactive free radicals, metal and semiconductor clusters, and bimolecular transition states.[1–5] Negative ions can be mass-selected prior to spectroscopic investigation and selection rules for photodetachment versus excitation of a neutral molecule are drastically relaxed. However, the resolution of PES is at best 5–10 meV, sufficient to resolve electronic and some vibrational structure but not the low frequency vibrations that occur in many molecules and clusters. Anion zero electron-kinetic-energy (ZEKE) spectroscopy,[6–8] a detection scheme which provides a spectral resolution of a few cm^{-1}, is experimentally very challenging, and one is limited to the investigation of species where the electron leaves as an *s* wave. This paper presents a technique that combines the advantages of PES and ZEKE by using velocity map imaging (VMI) to collect photoelectrons with low but nonzero kinetic energy at a collection efficiency of ≈100%. We demonstrate the advantages of this method compared to conventional PES and anion ZEKE spectroscopy through its application to I^-, $I^-(CO_2)$, and $Cl^-(D_2)$; photodetachment of the third species is of particular interest as it probes the open-shell van der Waals cluster $Cl \cdot D_2$, which plays an important role in the $Cl + D_2$ reaction.[9]

The three techniques are compared in Fig. 1. Conventional anion PES [Fig. 1(a)] is typically performed at a single photodetachment wavelength; measurement of the resulting electron kinetic energy (eKE) distribution [dashed arrows in Fig. 1(a)] then maps out the electronic and vibrational levels of the neutral species formed by photodetachment. The information obtained from conventional PES is often limited by the resolution of the electron energy analyzer which, in the best cases, amounts to 5–10 meV and is often considerably lower. The highest resolution is generally achieved using hemispherical analyzers or field free time-of-flight measurements, both of which have low photoelectron collection efficiency.

In anion ZEKE spectroscopy [Fig. 1(b)],[6] mass-selected anions are photodetached with a tunable pulsed laser, and only those electrons with nearly zero kinetic energy are collected as the laser is scanned. ZEKE signal is seen when the laser passes through a photodetachment threshold between an anion and neutral level. Because only a very small range of kinetic energies [shaded areas in Fig. 1(b)] is collected at each laser wavelength, many small energy steps are required to record a full spectrum. The energy resolution can be as high as 1 cm^{-1}, but ZEKE spectra of most molecular anions have features at least 8–10 cm^{-1} wide owing to unresolved rotational structure. In anion ZEKE experiments, the near ZEKE and higher energy electrons are allowed to separate spatially for ~200 ns after the laser pulse fires, after which a weak pulsed electric field is applied to extract and detect the slow electrons; selective detection of the ZEKE electrons is achieved by a combination of spatial and temporal filtering. The physics of anion ZEKE are quite different than in neutral ZEKE experiments, which are now understood to involve pulsed field ionization of very high Rydberg states.[10] The near-zero energy electrons produced in the anion experiments are extremely sensitive to stray electric and magnetic fields, making these experiments quite difficult. In addition to the experimental difficulties, anion ZEKE is further complicated by the Wigner threshold law[11] which predicts the photodetachment cross-section σ to be $\sigma \propto (h\nu - E_{th})^{\ell + 1/2}$, where $h\nu - E_{th}$ is the energy difference between the photodetachment laser and detachment threshold, and ℓ is the angular momentum of the photoelectron. Clearly, σ is always zero at threshold and increases rapidly with photon energy only if ℓ is zero (*s*-wave scatterers). For all systems with $\ell > 0$, σ remains close to zero for an energy range of several meV above threshold, thereby preventing the recording of a ZEKE spectrum.

[a)]Author to whom correspondence should be addressed. Electronic mail: dan@radon.cchem.berkeley.edu

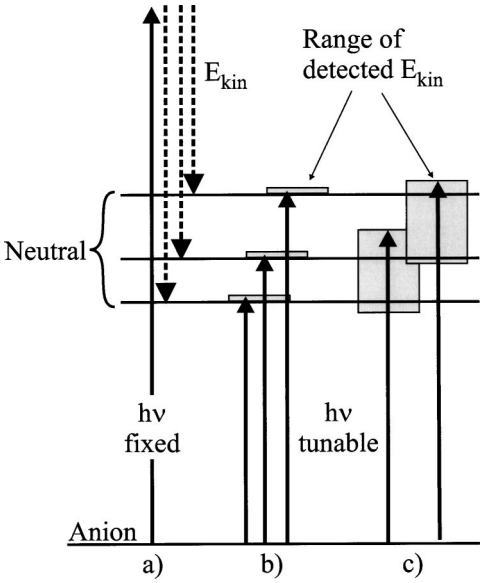

FIG. 1. Schemes for (a) conventional photoelectron spectroscopy (PES), (b) anion zero electron kinetic energy (ZEKE) spectroscopy, and (c) slow electron velocity map imaging (SEVI).

The experiment described in this paper is based on the VMI of slow photoelectrons; slow electron velocity-map imaging (SEVI) [Fig. 1(c)]. Anions are photodetached in a dc electric field which projects the photoelectron velocity distribution onto a detector coupled to a phosphor screen; the resulting image is recorded using a CCD camera, and analyzed to yield photoelectron eKE and angular distributions. Photoelectron VMI has been used in several laboratories[12–16] including ours, as an alternate technique for performing PES on neutrals and anions. The technique has yielded a fractional energy resolution $\Delta E/eKE$ as low as 2% (Ref. 17) and high collection efficiency, especially for the lowest energy electrons.

A typical VMI experiment employs dc fields in the photodetachment region that are sufficiently high to collect all photoelectrons, regardless of their kinetic energy. In our experiment, considerably lower extraction fields are used, so that only photoelectrons with eKE of ~10–20 meV or less are collected with near unit efficiency. At eKE=10 meV, the highest resolution achieved in photoelectron imaging corresponds to an energy resolution of better than 2 cm^{-1}. By scanning the photodetachment laser in steps on the order of 10 meV, one obtains a series of very high resolution photoelectron spectra that each shows a large range of eKE [shaded areas in Fig. 1(c)]. Hence, SEVI is somewhat of a hybrid of conventional PES in which only a single laser wavelength is used, and anion ZEKE in which the laser is continuously tuned. As will be shown, SEVI yields spectra comparable in resolution to anion ZEKE spectra but with much shorter data acquisition times. Moreover, since the detachment laser is typically several meV above a detachment threshold, it should be possible to observe *p*-wave detachment, although we have not yet done so. Our experiment draws upon photoionization and photodetachment microscopy experiments reported previously by Vrakking,[18,19] Blondel,[20,21] and co-workers; those experiments were more concerned with measuring interference effects associated with extremely slow electrons, rather than as a means of carrying out high resolution photoelectron spectroscopy over an extended energy range.

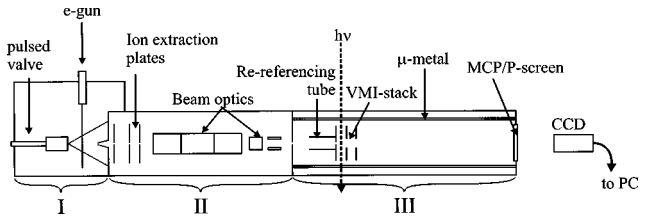

FIG. 2. The experimental setup used for the present experiments (not to scale). Regions I-III are the source region (I), the extraction and ion beam manipulation region (II), and the excitation and detection region (III).

In this paper we report results for two ions, I^- and $I^-(CO_2)$, which have previously been studied by anion ZEKE spectroscopy and therefore serve as test systems for the SEVI experiment.[6,22] Results are then presented for $Cl^-(D_2)$, for which the photoelectron spectrum was previously reported.[23] The PE spectrum showed no structure other than that associated with the spin-orbit splitting of the Cl atom, but the SEVI spectrum shows partially resolved features assigned to a hindered rotor progression in the $Cl\cdot D_2$ van der Waals complex.

II. EXPERIMENT

Experiments take place in a multiply-differentially pumped chamber (shown in Fig. 2) that is divided into a source region (labeled I in the figure), a beam acceleration/manipulation region (II), and an excitation/detection region (III). For the production of anions, a suitable precursor gas is expanded through a 20 Hz-pulsed piezo valve at stagnation pressures in the range of 20–80 psi. Precursor gases for the present experiments were composed of traces of CF_3I in Ar or in a 1:2 mixture of CO_2 in Ar [spectroscopy of I^- and $I^-(CO_2)$, respectively], and traces of CCl_4 in a 5:1 Ar/D_2 mixture [spectroscopy of $Cl^-(D_2)$]. The expansion is crossed perpendicularly by a 1 keV, ~200 μA electron beam from a continuous electron gun. Anions are formed through attachment of secondary electrons from electron impact ionization to fragments of the precursor molecules. Only the central part of the ion beam enters the second region through a skimmer with a 1–2 mm orifice.

The anions are accelerated and mass separated in a collinear mass spectrometer. Two types of mass spectrometers have been employed in the present studies: for the experiments on I^- and $I^-(CO_2)$, the ions were extracted in a Bakker-type mass spectrometer,[24,25] and the $Cl^-(D_2)$ work was done using the collinear Wiley McLaren-type mass spectrometer[26] shown in Fig. 2. The latter configuration yields increased signal by about a factor of 2 along with considerably better stability. Ions are focused and steered through the pinholes into the VMI region by a cylindrical Einzel-lens and by sets of vertical and horizontal deflectors. Upon entering the excitation region, the ion packets are compressed to ~50 ns, corresponding to a mass resolution $M/\Delta M = 400$.

The VMI region is entered through a re-referencing tube that is grounded when the ions enter but switched to the desired negative voltage while the selected ion packet is inside. This configuration is necessary to allow collinear electron extraction without the need of pulsed imaging. The design of the VMI region is similar to the one employed in the original work by Eppink and Parker:[27] the three plates (repeller, extraction, and ground plate) are spaced by 1.5 cm each, the extraction and ground plates have holes with a 2.54 cm (1 in.) diameter, while the repeller plate has a pinhole with a 3 mm diameter. The laser is focused between the repeller and extraction plates, and propagates perpendicularly to the molecular beam axis, with a polarization vector parallel to the imaging plane. Photoelectrons are accelerated toward the imaging detector in the dc fields obtained by applying voltages to the first two plates, and the electron clouds generated from the different detachment thresholds expand on the way to the detector. A time gate on the detector insures that only photoelectrons from the laser pulse are detected; these arrive at the detector considerably earlier than the ions that survive the detachment laser pulse.

Because the threshold photoelectrons expand only slowly, high-resolution SEVI requires long flight times. In the present experiment, a 1 m long flight tube is used in combination with repeller voltages generally in the range 50–200 V. The use of higher voltages allows the operation of the experiment in a low-resolution mode by extracting electrons with eKE up to ~150 meV. As a result of the low extraction voltages, the photoelectrons are very sensitive to stray electric and magnetic fields and special precautions have to be taken in order to obtain unperturbed images. Particular care has been taken to reduce stray electric fields in the VMI region where perturbations of the slow electron-trajectories have the strongest effects. The polished stainless steel plates possess rims that extend from each plate to half way between neighboring plates such that fields from surrounding cables and connections are blocked. Additionally, these rims improve the quality of the electric fields between the plates. Electric fields from the high-voltage connections to the imaging microchannel plates (MCP) and the phosphor screen are blocked by mounting a grounded steel disk directly in front of the MCP. Magnetic fields are avoided by shielding the complete excitation and detection region by two concentric μ-metal tubes. Photoelectrons hitting the 75 mm diameter MCP produce an image on the phosphor screen, which is recorded with a CCD camera and transferred to a PC for work-up and analysis.

The collinear VMI arrangement in Fig. 2 is similar to that used in our time-resolved imaging experiments,[15] but the ion lens voltages are considerably lower here, because we are only interested in collecting relatively low-energy photoelectrons. The collinear configuration presents some experimental difficulties compared to the perpendicular VMI arrangement used by other groups in studies of negative ions,[12,13] but offers the significant advantage that its energy resolution is, to first order, independent of the spread in ion beam energy induced by the time-of-flight mass spectrometer, a crucial point in the experiments presented here where we are trying to achieve the highest resolution possible.

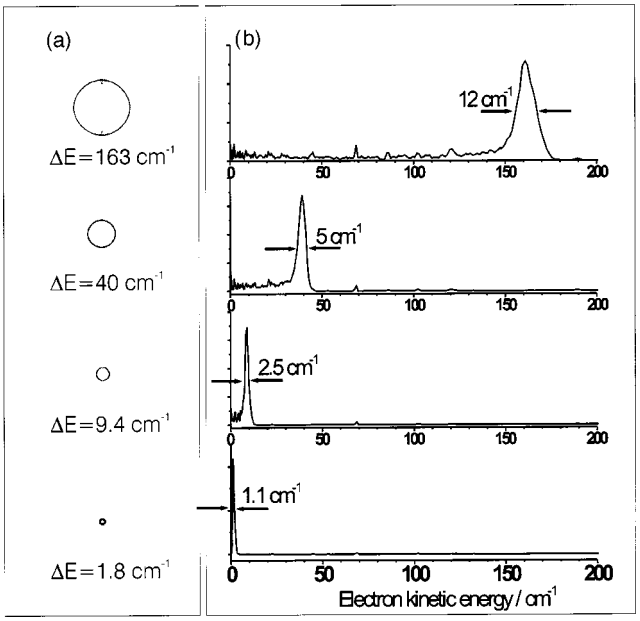

FIG. 3. SEVI spectra of atomic iodide at electron kinetic energies of 163 cm^{-1}, 40 cm^{-1}, 9.4 cm^{-1}, and 1.8 cm^{-1} (from top to bottom). Panel (a) shows the photoelectron images after inverse Abel transformation, the traces in panel (b) are the angular integrations of the corresponding images.

III. RESULTS AND DISCUSSION

Figure 3(a) shows a series of photoelectron images taken from photodetachment of I^- at laser energies (from top to bottom) of 163, 40, 9.4, and 1.8 cm^{-1} above the detachment threshold to the $I(^2P_{3/2})$ state, for which the electron affinity (EA) is 3.059 eV.[28] Photoelectron spectra obtained by angular integration of the images are shown in Fig. 3(b). Because the electric fields employed for the velocity mapping were the same for all spectra shown in Fig. 3, 100 V on the repeller plate and 70 V on the extraction plate, the size of the image gradually decreases as $eKE = h\nu - EA$ is reduced. At the same time, the constant resolution of the images in velocity-space is reflected in a reduced linewidth at lower kinetic energies: the images displayed in Fig. 3(a) are each ~6–8 pixels wide, which corresponds to a peak width of 1.1 cm^{-1} at eKE=1.8 cm^{-1} and 12 cm^{-1} at eKE=163 cm^{-1}. As the eKE increases, the fractional energy resolution $\Delta E/eKE$ improves but then gets worse as the fastest electrons approach the edge of the imaging detector where stray fields from the MCP and phosphor screen voltages become noticeable and the images start to display deviations from perfect circular shapes. In Fig. 3, the smallest $\Delta E/eKE$, 7%, is found at eKE=163 cm^{-1} and corresponds to a peak width of 12 cm^{-1} (1.5 meV).

Sets of images like those displayed in Fig. 3 also serve to calibrate the detection method at a given choice of imaging fields. The precise eKE of the peak in each of these images is known from the electron affinity of iodine and the calibrated laser wave number. The kinetic energy is proportional to the square of the image radius and the proportionality factor has to be determined for each set of imaging voltages. The calibration was found to be stable over long periods of time and the resetting of the fields reproducible to within a sufficiently

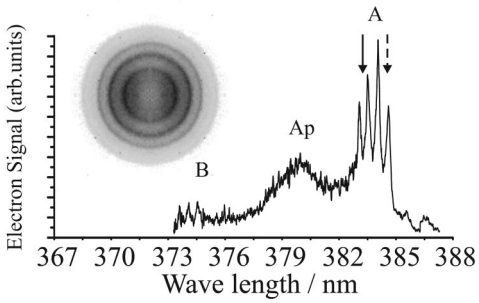

FIG. 4. SEVI spectrum of $I^-(CO_2)$. The insert shows the raw image obtained with the laser wavelength at 383.14 nm, indicated as a solid vertical arrow. The band origin is shown as a dashed vertical arrow.

high precision (i.e., effects of imperfect setting of the fields were smaller than the line width).

As a first application of SEVI to a molecular anion, we consider the species $I^-(CO_2)$. The PE and ZEKE spectra of this anion are known,[22,29] and its infrared spectrum has been recently reported.[30] The anion has a C_{2v} structure in which the CO_2 moiety is slightly bent, and its PE spectrum shows Franck-Condon activity in the high-frequency CO_2 bending mode of the neutral $I{\cdot}CO_2$ complex. The ZEKE spectrum shows considerably more structure, most notably a 30 cm^{-1} progression in the C-I stretch mode of $I{\cdot}CO_2$.

The SEVI spectrum of $I^-(CO_2)$ is displayed in Fig. 4. The insert shows a symmetrized raw image obtained with the laser set at 383.14 nm (indicated as a solid vertical arrow in Fig. 4). VMI voltages for this image were 150 V/107 V for the repeller and extraction plate, and 10 000 laser shots were accumulated. The image shows four well-resolved rings. The three innermost rings are spaced by 33 cm^{-1} and are part of a progression in the C-I stretch mode of $I{\cdot}CO_2$, while the outermost ring, separated by 65 cm^{-1} from the adjacent ring, corresponds to a hot band transition from the $v_{C\text{-}I}=1$ level of the anion.

The complete spectrum was obtained by joining together ten photoelectron spectra that were recorded with wavelength steps of 1.5 nm. At each wavelength, electrons from about 10 000 laser shots were accumulated, the image was Abel-inverted and the PES obtained from an angular integration was converted to electron kinetic energy by the procedure outlined in the last paragraph. Overlap between adjacent spectra was used for intensity normalization. Bands A, Ap, and B in Fig. 4 result from excitation of $I(^2P_{3/2}){\cdot}(CO_2)$ with zero (bands A and Ap) and one (band B) quantum of CO_2 bend excitation. The splitting of the low-energy band in two sub-bands A and Ap has its origin in two possible values of Ω ($\Omega=1/2$ and 3/2), the projection of the total angular momentum of the iodine atom on the axis connecting the center-of-mass of CO_2 with I.[31] The progression of peaks in the image appears in band A of the complete spectrum; a similar, lower intensity progression also appears in band B.

The resolution in the SEVI spectrum is slightly lower than in the ZEKE spectrum,[22] but the clear advantage of the new experiment is in the greatly reduced data acquisition time: while the ZEKE spectrum was recorded by scanning the laser in steps of 0.005 nm and accumulating 5000 laser shots at each wavelength, the SEVI spectrum required only ten images and 10 000 laser shots at each wavelength. The total data acquisition time was thus reduced from many days to 2 h.

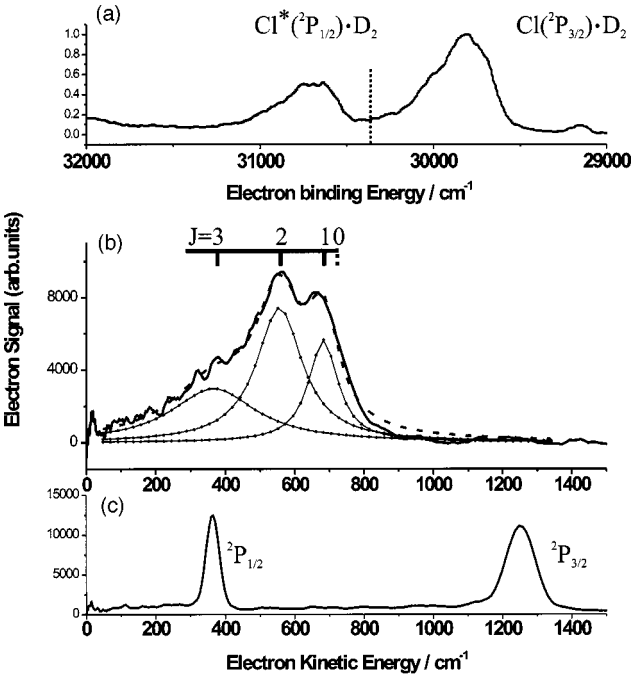

FIG. 5. Panel (a) PES of $Cl^-(D_2)$ showing the two clusters of transitions due to the two spin-orbit levels of Cl. The dotted vertical line indicates the origin of the energy axes in Panels (b) and (c). (b) SEVI-spectrum of $Cl(^2P_{3/2})\cdot D_2$. The three Lorentzian lines used to fit the spectrum and their sum are shown as dotted and dashed lines, respectively. (c) SEVI-spectrum of Cl recorded under the same conditions as the $Cl{\cdot}D_2$ spectrum. In all panels, the electron binding energy increases from right to left.

Finally, SEVI was applied to the $Cl^-(D_2)$ anion. This species and $Cl^-(H_2)$ were studied previously by Wild *et al.*,[32,33] who measured rotationally-resolved infrared spectra, and by Ferguson *et al.*[23] who measured their photoelectron spectra. Theoretical studies[34,35] have shown the anion to have a linear geometry and a dissociation energy of 500–600 cm^{-1}, depending on the isotope under consideration, in general agreement with the conclusions of Wild *et al.* These anions are of considerable interest because photodetachment accesses the shallow minimum [0.5 kcal/mol (Ref. 36)] on the $Cl+H_2$ potential energy surface corresponding to the open shell $Cl{\cdot}H_2$ van der Waals complex, which in turn has been shown to play an important role in the overall $Cl+H_2$ reaction dynamics.[9] Anion photoelectron spectroscopy thus offers the opportunity to probe the vibrational, electronic, and (possibly) the rotational structure of the open-shell complex, and better characterize its role in the bimolecular reaction.

The previously measured photoelectron spectrum of $Cl^-(D_2)$ is shown in Fig. 5(a). It shows two main features, which are spaced by the spin-orbit splitting in atomic Cl, 879 cm^{-1} (0.109 eV), and correspond to transitions to the $Cl(^2P_{3/2})\cdot D_2$ and $Cl^*(^2P_{1/2})\cdot D_2$ levels of the neutral complex. The spectrum shows hints of unresolved structure contributing to both the peaks, as both transitions are wider than in $Cl^-(H_2)$.[23] The possibility of resolving this structure

makes $Cl^-(D_2)$ an attractive target for our SEVI experiment.

Figure 5(b) shows the SEVI spectrum of $Cl^-(D_2)$, taken at a laser wave number of 30 385.1 cm^{-1}, indicated as a dotted vertical line in panel (a). Only the $Cl(^2P_{3/2})\cdot D_2$ feature is accessible at this photon energy. The VMI voltages were $V(\text{repeller})=918$ V and $V(\text{extraction})=656$ V. These relatively high settings allowed collection of the entire $Cl(^2P_{3/2})\cdot D_2$ feature; no additional structure was seen at lower voltages. The spectrum of atomic chloride, recorded under the same conditions as Fig. 5(b), is shown in Fig. 5(c) for comparison. We observe two partially resolved transitions and a tail toward low eKE. The spacing between the two features, 126 cm^{-1}, is similar to the splitting between the $J=1$ and 2 rotational levels of D_2. Moreover, the entire spectrum can be fit assuming it comprises three Lorentzian lines with center energies and linewidths Γ(full width at half maximum) of eKE=366 cm^{-1} ($\Gamma=295$ cm^{-1}), 555 cm^{-1} ($\Gamma=161$ cm^{-1}), and 681 cm^{-1} ($\Gamma=102$ cm^{-1}), respectively. The resulting transitions are shown as dotted lines in the same figure and the sum is represented as a dashed line. The splitting between the two transitions at lower eKE, 189 cm^{-1}, is close to the spacing between the $J=2$ and 3 rotational levels of D_2.

It thus appears we are observing a progression in hindered rotor levels of the $Cl\cdot D_2$ complex. Such an interpretation is reasonable in light of our previous observation of a similar progression in the photoelectron spectrum of $F^-(para\text{-}H_2)$;[37] in both cases, the interaction between the halogen and hydrogen molecule in the region of the neutral surface accessed by photodetachment is too weak to perturb the molecular rotational energy levels beyond the experimental resolution. Recent simulations of the $Cl\cdot D_2$ spectrum by Alexander[38] offer further support for this assignment. Note that there may be a $J=0$ component to this progression, but it cannot be resolved in our spectrum.

The origin of the trend in the Lorentzian linewidths is of interest, because the $Cl\cdot D_2$ complex is very weakly bound, and the deposition of internal energy is likely to promote dissociation to $Cl+D_2$. On the other hand, there should be additional, finer structure in the spectra other than the observed hindered rotor progression. The $Cl(^2P_{3/2})$ level is split into two closely-spaced components owing to its interaction with the H_2 molecule; while this splitting has not been determined experimentally for $Cl\cdot H_2$, it is known to be 37 cm^{-1} in $Cl\cdot Ar$.[39] In addition, one expects a progression in the low frequency Cl-H_2 stretching mode. The results by Alexander[38] suggest that the effective linewidths in our spectra are largely due to unresolved underlying structure of the type just described. However, homogeneous broadening from lifetime effects becomes significant when the Cl-D_2 stretch is excited with two or more quanta, a reasonable result since this mode is directly coupled to dissociation.

Overall, it appears that we are thus far only resolving hindered rotor structure in the $Cl\cdot D_2$ complex, but that additional structure should be present and observable, either by improving the experimental resolution or by reducing the density of neutral vibration-rotation states. The latter can be accomplished by investigations of $Cl^-(H_2)$, where the hindered rotor levels will be more widely spaced, and by incorporating either $para$-H_2 or $ortho$-D_2 into the anion complexes, which will eliminate half the hindered rotor levels seen in the photodetachment spectrum.[37,40] Nonetheless, the new data presented here represent a step towards a full understanding of the entrance valley of the $Cl+H_2$ reaction in the region close to the transition state.

IV. SUMMARY

We have presented a technique, SEVI, for high-resolution anion-photoelectron spectroscopy. The technique uses velocity-map imaging to overcome some of the most fundamental problems of the original anion-ZEKE technique. As a result we obtain at the same time high sensitivity, high resolution, and fast data acquisition. The performance of SEVI was tested on atomic iodide and $I^-(CO_2)$, both of which had been studied previously using ZEKE spectroscopy. The SEVI spectrum of $Cl^-(D_2)$ reveals hindered rotor structure of the $Cl\cdot D_2$ open shell van der Waals complex.

ACKNOWLEDGMENTS

Support by the Air Force Office for Scientific Research under Grant No. F49620-03-1-0085 is gratefully acknowledged. A.O. thanks the Swiss National Science Foundation for a postdoctoral fellowship. The authors thank M. Alexander and D. Manolopoulos for providing unpublished data on the $Cl\cdot D_2$ complex.

[1] K. M. Ervin and W. C. Lineberger, in *Advances in Gas Phase Ion Chemistry*, edited by L. M. Babcock (JAI, Greenwich, 1992), Vol. 1, pp. 121–166.
[2] O. Cheshnovsky, S. H. Yang, C. L. Pettiette, M. J. Craycraft, Y. Liu, and R. E. Smalley, Chem. Phys. Lett. **138**, 119 (1987).
[3] D. M. Neumark, Accts. Chem. Res. **26**, 33 (1993).
[4] H. B. Wu, S. R. Desai, and L. S. Wang, Phys. Rev. Lett. **77**, 2436 (1996).
[5] D. M. Neumark, Phys Chem Comm **5**, 76 (2002).
[6] T. N. Kitsopoulos, I. M. Waller, J. G. Loeser, and D. M. Neumark, Chem. Phys. Lett. **159**, 300 (1989).
[7] G. F. Gantefor, D. M. Cox, and A. Kaldor, J. Chem. Phys. **93**, 8395 (1990).
[8] C. Bassmann, U. Boesl, D. Yang, G. Drechsler, and E. W. Schlag, Int. J. Mass Spectrom. Ion Processes **159**, 153 (1996).
[9] D. Skouteris, D. E. Manolopoulos, W. S. Bian, H. J. Werner, L. H. Lai, and K. P. Liu, Science **286**, 1713 (1999).
[10] T. P. Softley, Int. Rev. Phys. Chem. **23**, 1 (2004).
[11] E. P. Wigner, Phys. Rev. **73**, 1002 (1948).
[12] B. Baguenard, J. C. Pinare, C. Bordas, and M. Broyer, Phys. Rev. A **63**, 023204 (2001).
[13] E. Surber and A. Sanov, J. Chem. Phys. **116**, 5921 (2002).
[14] E. Surber, R. Mabbs, and A. Sanov, J. Phys. Chem. A **107**, 8215 (2003).
[15] A. V. Davis, R. Wester, A. E. Bragg, and D. M. Neumark, J. Chem. Phys. **118**, 999 (2003).
[16] D. S. Peterka, A. Lindinger, L. Poisson, M. Ahmed, and D. M. Neumark, Phys. Rev. Lett. **91**, 043401 (2003).
[17] M. J. J. Vrakking, Rev. Sci. Instrum. **72**, 4084 (2001).
[18] C. Bordas, F. Lepine, C. Nicole, and M. J. J. Vrakking, Phys. Rev. A **68**, 012709 (2003).
[19] C. Nicole, H. L. Offerhaus, M. J. J. Vrakking, F. Lepine, and C. Bordas, Phys. Rev. Lett. **88**, 133001 (2002).
[20] C. Blondel, C. Delsart, F. Dulieu, and C. Valli, Eur. Phys. J. D **5**, 207 (1999).
[21] C. Delsart, F. Goldfarb, and C. Blondel, Phys. Rev. Lett. **89**, 183002 (2002).
[22] Y. X. Zhao, C. C. Arnold, and D. M. Neumark, J. Chem. Soc., Faraday Trans. **89**, 1449 (1993).
[23] M. J. Ferguson, G. Meloni, H. Gomez, and D. M. Neumark, J. Chem. Phys. **117**, 8181 (2002).
[24] J. M. B. Bakker, J. Phys. E **6**, 785 (1973).
[25] J. M. B. Bakker, J. Phys. E **7**, 364 (1974).
[26] W. C. Wiley and I. H. McLaren, Rev. Sci. Instrum. **26**, 1150 (1955).

[27] A. T. J. B. Eppink and D. H. Parker, Rev. Sci. Instrum. **68**, 3477 (1997).
[28] D. Hanstorp and M. Gustafsson, J. Phys. B **25**, 1773 (1992).
[29] D. W. Arnold, S. E. Bradforth, E. H. Kim, and D. M. Neumark, J. Chem. Phys. **102**, 3510 (1995).
[30] J. M. Weber and H. Schneider, J. Chem. Phys. **120**, 10056 (2004).
[31] A. Sanov, J. Faeder, R. Parson, and W. C. Lineberger, Chem. Phys. Lett. **313**, 812 (1999).
[32] D. A. Wild, R. L. Wilson, P. S. Weiser, and E. J. Bieske, J. Chem. Phys. **113**, 10154 (2000).
[33] D. A. Wild, P. S. Weiser, E. J. Bieske, and A. Zehnacker, J. Chem. Phys. **115**, 824 (2001).
[34] M. H. Alexander, J. Chem. Phys. **118**, 9637 (2003).
[35] A. A. Buchachenko, T. A. Grinev, J. Klos, E. J. Bieske, M. M. Szczesniak, and G. Chalasinski, J. Chem. Phys. **119**, 12931 (2003).
[36] W. S. Bian and H. J. Werner, J. Chem. Phys. **112**, 220 (2000).
[37] D. E. Manolopoulos, K. Stark, H. J. Werner, D. W. Arnold, S. E. Bradforth, and D. M. Neumark, Science **262**, 1852 (1993).
[38] D. Manolopoulos and M. Alexander, (private communication).
[39] T. Lenzer, I. Yourshaw, M. R. Furlanetto, G. Reiser, and D. M. Neumark, J. Chem. Phys. **110**, 9578 (1999).
[40] S. E. Bradforth, D. W. Arnold, D. M. Neumark, and D. E. Manolopoulos, J. Chem. Phys. **99**, 6345 (1993).